

ATOMISTIC POTENTIALS AND THE CAUCHY-BORN RULE FOR CARBON NANOTUBES: A REVIEW

MANUEL FRIEDRICH, EDOARDO MAININI, AND PAOLO PIOVANO

ABSTRACT. Carbon nanotubes are modeled as point particle configurations in the framework of Molecular Mechanics, where interactions are described by means of short range attractive-repulsive potentials. The identification of local energy minimizers yields a variational description for the stability of rolled-up hexagonal-lattice structures. Optimality of periodic configurations is preserved under moderate tension, hence justifying the elastic behavior of carbon nanotubes in the axial traction regime.

1. INTRODUCTION

Carbon nanotubes are long cylindrical structures made of atom-thick layers of carbon atoms forming sp^2 covalent bonds and locally arranging themselves in hexagonal-lattice patterns [9, 14]. Among the reasons of the central role that carbon nanotubes have conquered in several modern technology applications, we mention their exceptional mechanical properties and tensile strength [3, 24, 41], and the fact that they can grow in length up to 10^8 times the diameter [45, 51].

The mechanical response of nanotubes under *stretching* is therefore a topical research subject from the theoretical [4, 16, 35, 36, 46, 50], the computational [1, 7, 22, 23], and the experimental point of view [13, 24, 26, 43, 48, 49]. Ab initio models from quantum mechanics provide an accurate description of the atomic scale and may describe characterizing features of carbon nanotube geometry and mechanics [27, 34, 47]. The drawback of these methods is the rapid increase in computational complexity. Hence, for large systems, it is suitable to consider a description in the framework of molecular mechanics [2, 25, 33], thus regarding atoms as classical interacting point particles.

Following the latter approach, we identify carbon nanotubes with configurations $\{x_1, \dots, x_n\} \in \mathbb{R}^{3n}$ corresponding to atomic positions. The atoms interact via *configurational energies* $E = E(x_1, \dots, x_n)$ that depend on the mutual positions of particles and are consistent with the phenomenology of sp^2 covalent bonding. The energy features classical potentials taking into account both attractive-repulsive *two-body* effects, minimized at a certain atomic distance, and *three-body* terms favoring specific angles between bonds [5, 37, 38, 39, 40]. The sp^2 -type covalent bonding implies that each atom has exactly three first neighbors and that bond angles of $2\pi/3$ are energetically preferred [9]. Similar potentials have been previously employed to describe also other carbon allotropes, e.g., graphene in [12, 20, 30] and fullerene C_{60} in [19].

In this paper we review the analytical results from [18, 28, 29]: We study the local minimality of periodic configurations, both in the unstretched case and under the effect of small axial stretching. More specifically, we prove that, by applying a small stretching to a nanotube, the energy E is locally strictly minimized by a specific periodic configuration where all atoms see the same local configuration (see Theorem 3.4 below). Local minimality is here assessed with respect to *all* small perturbations in \mathbb{R}^{3n} , namely not restricting *a priori* to only periodic perturbations. On the contrary, periodicity is shown to emerge as a byproduct of our variational analysis. This results provides new motivation for the continuum mechanics approaches to carbon nanotubes and opens the possibility of developing a discrete-to-continuum theory. In this regard, we refer the reader to the various continuum models provided in the literature such as [3, 4, 15, 17, 32, 35, 42].

2010 *Mathematics Subject Classification.* Primary: 82D25.

Key words and phrases. Carbon nanotubes, Tersoff energy, variational perspective, stability, Cauchy-Born rule.

Our result can be seen as a validation of the so-called *Cauchy-Born rule* for carbon nanotubes: By imposing a small tension, the periodicity cell deforms correspondingly so that the deformation at the microscale is uniformly distributed along the sample. In other words, atoms follow the macroscopic deformation and microscopic periodicity is preserved under imposing a macroscopic stretching. We stress that such periodicity is invariably *assumed* in a number of different contributions, see [4, 16, 22, 50] among others, and then exploited in order to compute tensile strength as well as stretched geometries. Here again our results provide a theoretical justification of such approaches.

Let us mention that, in principle, the Cauchy-Born rule would require to check the elastic behavior of the structure with respect to any imposed small displacement. However, we limit ourselves to consider the most natural tensile stress experiment for the nanotube, i.e., the uniaxial traction. In this setting, we prove that in the small deformation regime, there exists a local minimizer of the energy in which the microscopic periodical pattern is preserved. This seems to be the strongest result one can aim for in our context, as *global minimality* is not expected in general for nanotubes and could be instead achieved by completely different topologies. For example, under not too restrictive hypotheses on the three-body terms, structures corresponding to the sp^3 hybridization such as diamonds (which display four nearest neighbors for each bulk atom, arranged at the vertices of a tetrahedron) are energetically favored (see [30] for more details in this direction).

Finally, we notice that various technical difficulties in the proof originate exactly from the fact that our configurational energy is tailored to describe covalent sp^2 bonds. Indeed, in principle, such modeling assumptions are meant to describe the local minimality of planar configurations, such as graphene [30] and graphene nanoflakes [12]. When introducing rolled-up structures, however, the non-planarity effect destroys the local optimality around each point. Only a very careful study of the global geometric constraint given by the rolling-up allows to still identify specific nanotube configurations as local minimizers.

The paper is organized as follows: In Section 2 we introduce a precise geometric description of carbon nanotubes along with the definition of the configurational energy. In Section 3 we state the main result. In Section 4 we collect the main auxiliary tools and we provide a summary of the proof of the main result.

2. GEOMETRIC AND VARIATIONAL DESCRIPTION OF CARBON NANOTUBES

2.1. Geometry of zigzag nanotubes. For a precise geometric description, we start from some distinguished and highly symmetric configurations related to *zigzag* nanotubes. The term *zigzag* refers to a particular nanotube geometry depicted in Figure 2 that ideally results from rolling up graphene sheets along specific axis directions suitably chosen with respect to the lattice vectors of the planar honeycomb graph of the graphene sheet, see Figure 1. However, we notice that the definitions introduced here can be easily adapted to other classical choices, namely the *armchair* geometry, where the axis of the cylinder is instead orthogonal to the bisector of the planar lattice vectors. We refer to [29] for a precise geometric description in the armchair case.

We let $\ell \in \mathbb{N}$, $\ell > 3$, and define the family \mathcal{F} of zigzag nanotubes as the collection of all configurations that, up to isometries, coincide with the set of points

$$\left(k(\lambda_1 + \sigma) + j(2\sigma + 2\lambda_1) + l(2\sigma + \lambda_1), \rho \cos\left(\frac{\pi(2i+k)}{\ell}\right), \rho \sin\left(\frac{\pi(2i+k)}{\ell}\right) \right), \quad (1)$$

$i = 1, \dots, \ell$, $j \in \mathbb{Z}$, $k, l \in \{0, 1\}$, for some choice of

$$\lambda_1 \in (0, \mu/2), \quad \lambda_2 \in (0, \mu/2), \quad \sigma \in (0, \mu/2), \quad \text{and} \quad \rho \in \left(0, \frac{\mu}{4 \sin(\pi/(2\ell))}\right)$$

satisfying the constraints

$$2\sigma + 2\lambda_1 = \mu, \quad \sigma^2 + 4\rho^2 \sin^2\left(\frac{\pi}{2\ell}\right) = \lambda_2^2. \quad (2)$$

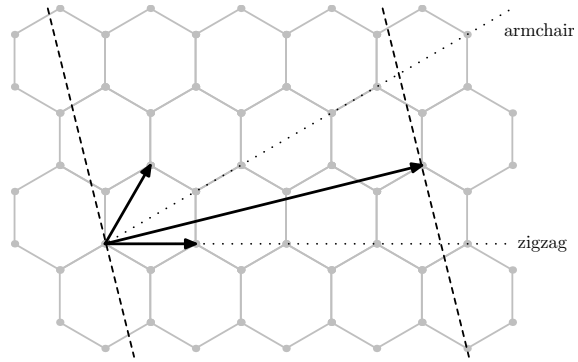


FIGURE 1. Rolling-up of a graphene sheet: a zigzag nanotube is the result of rolling up in such a way that the axis of the cylinder is orthogonal to one of the lattice vectors.

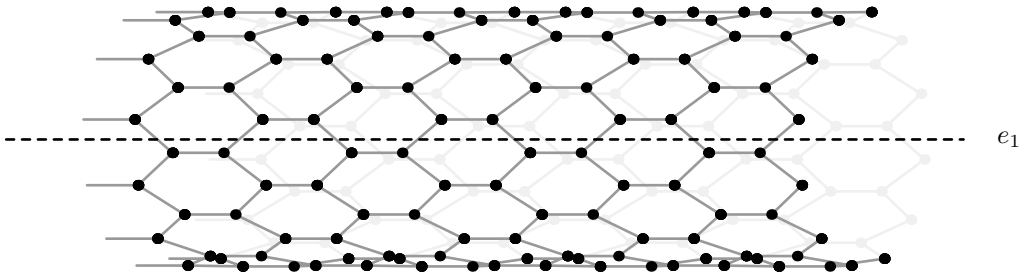


FIGURE 2. Zigzag nanotube.

The parameter ρ indicates the diameter of the tube and λ_1, λ_2 are the two possibly different lengths of the covalent bonds in each hexagon of the tube, where the bonds of length λ_1 are oriented in the \mathbf{e}_1 direction (see Figure 3). The parameter μ represents instead the minimal period. We stress that, in the above definition, the only parameter that is fixed a-priori is the number ℓ of atoms per section, and that by (2) we can see \mathcal{F} as a three-parameter family depending on λ_1, λ_2 and μ . In the following we denote a generic configuration in \mathcal{F} by \mathcal{F} and, when we want to refer to the particular parameters λ_1, λ_2 , and μ that uniquely determine such configuration we use the notation $\mathcal{F}_{\lambda_1, \lambda_2, \mu}$. Furthermore, the one-parameter subfamily of all configurations characterized by unitary bonds, namely the collection of all configurations $\mathcal{F}_{1,1,\mu} \in \mathcal{F}$ for admissible μ , will be denoted by \mathcal{F}_1 .

We observe that any configuration $\mathcal{F} \in \mathcal{F}$ is periodic in the axis direction, and it is not difficult to check that it enjoys the following properties: Atoms in \mathcal{F} both lie on the surface of a cylinder with radius ρ (we denote the direction of the axis of the cylinder by \mathbf{e}_1), and are arranged in planar sections, perpendicular to \mathbf{e}_1 , obtained by fixing j, k , and l in (1). Each of the sections contains exactly ℓ atoms, arranged at the vertices of a regular ℓ -gon. For each section, the two closest sections are at distance σ and λ_1 , respectively.

We shall impose restrictions to the range of the parameters in order to avoid degeneracy of the structure. In particular, we shall impose that each atom has exactly three and only three neighbors at distance less than a reference value chosen as 1.1 in accordance to the fact that only atoms closer than 1.1 contribute to the energy that we define later on in Subsection 2.2. This can be ensured by some simple trigonometry which yields suitable explicit bounds on the parameters. We do not give detail about this, apart from noticing that the bond lengths λ_1 and λ_2 will lie in a neighborhood of the reference value 1, the parameter μ will lie in a neighborhood of 3, and the bond angles will lie in a neighborhood of $2\pi/3$, which are the values of the perfect unit planar

hexagonal lattice (to which we are locally close for very large ℓ). For instance, $\lambda_1, \lambda_2 \in (0.9, 1.1)$ and $\mu \in (2.6, 3.1)$ are fine choices, see [18].

If we denote by α the two angles that are adjacent to a bond in the axis direction and by β the remaining angles (see also Figure 3), we have the obvious relation $2\alpha + \beta < 2\pi$. Some more simple trigonometry (see [29, 18]) shows that

$$\sin \alpha = \sqrt{1 - (\sigma/\lambda_2)^2} = 2(\rho/\lambda_2) \sin\left(\frac{\pi}{2\ell}\right) \quad (3)$$

and that

$$\beta = \beta(\alpha, \gamma_\ell) := 2 \arcsin\left(\sin \alpha \sin \frac{\gamma_\ell}{2}\right), \quad (4)$$

where γ_ℓ is the internal angle of a regular 2ℓ -gon, i.e.,

$$\gamma_\ell := \pi \left(1 - \frac{1}{\ell}\right). \quad (5)$$

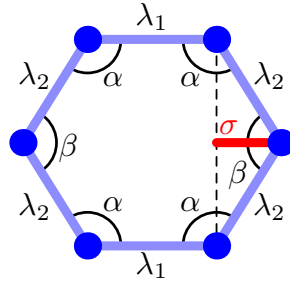


FIGURE 3. The bond lengths and the angles for the hexagon of a configuration in \mathcal{F} are represented. A segment representing σ (lying on the horizontal diagonal) is drawn in red. The hexagon is in fact not planar but kinked along the horizontal diagonal.

2.2. Configurational energy. We shall define a *configurational energy* for collections of particles of the form $\mathcal{C} := C_n + L\mathbf{e}_1\mathbb{Z}$ where $L > 0$ plays the role of the macroscopic period of repetition of the n -sample $C_n := \{x_1, \dots, x_n\}$ of \mathcal{C} and \mathbf{e}_1 is a given direction in \mathbb{R}^3 . C_n is a collection of n points $x_i \in \mathbb{R}^3$ such that $x_i \cdot \mathbf{e}_1 \in [0, L)$. Any such generic configuration \mathcal{C} is characterized by its n -sample C_n and by L , so that we always identify \mathcal{C} with the couple (C_n, L) .

We now introduce the energy E for the configuration \mathcal{C} and we detail the hypotheses on E that we assume throughout the paper. We aim here at minimal assumptions in order to include in the analysis most of the choices that have been used for computational chemistry codes [6, 8, 21, 31, 44] and that have been proposed as empirical potentials for the description of covalent systems [5, 37, 38, 39, 40]. In particular, we will not give explicit forms for the energy, but only consider potential terms that satisfy some qualitative properties. This will lead to quite general results that are grounded only on natural symmetry, convexity, and monotonicity assumptions.

The energy E features *two-body* and *three-body* interactions among particles, that are respectively modeled by a potential v_2 favoring bonds between nearest neighbors of unitary length and a potential v_3 favoring angles of 120° between such bonds, see (6). This is consistent with the modeling of sp^2 covalent atomic bonding in carbon favoring a specific interatomic distance and angles of 120° .

We introduce the two-body potential $v_2 : (0, \infty) \rightarrow [-1, \infty)$, which is smooth and attains its minimum value only at 1 with $v_2(1) = -1$ and $v_2''(1) > 0$. Moreover, we ask v_2 to be *short-ranged*, i.e., to vanish after some reference value right to 1, say $v_2(r) = 0$ for $r \geq 1.1$. In this way, $x, y \in \mathcal{C}$ will contribute to the two-body term of the energy only if their distance is less than 1.1. Looking at the n -sample C_n and taking periodicity into account, this amounts to considering two

particles x_i and x_j of the n -cell C_n of \mathcal{C} as contributing to the two-body part of the energy only if $|x_i - x_j|_L < 1.1$, where $|\cdot|_L$ is the distance modulo L in the \mathbf{e}_1 direction defined by

$$|x_i - x_j|_L := \min_{t \in \{-1, 0, +1\}} |x_i - x_j + Lt\mathbf{e}_1|$$

for every $x_i, x_j \in C_n$. We also let $\mathcal{N} := \{(i, j) : x_i, x_j \in C_n, i \neq j, \text{ and } |x_i - x_j|_L < 1.1\}$ be the set of first-neighboring atoms.

We introduce the three-body potential $v_3 : [0, 2\pi] \rightarrow [0, \infty)$ and we assume that v_3 is smooth and symmetric around π , i.e., $v_3(\alpha) = v_3(2\pi - \alpha)$. Moreover, we suppose that the minimum value 0 of v_3 is attained only at $2\pi/3$ and $4\pi/3$ with $v_3''(2\pi/3) > 0$. We let $\mathcal{T} := \{(i, j, k) : i \neq k, (i, j) \in \mathcal{N} \text{ and } (j, k) \in \mathcal{N}\}$. For all triples $(i, j, k) \in \mathcal{T}$ we denote by $\alpha_{ijk} \in [0, \pi]$ the *bond angle* formed by the vectors $x_i - x_j$ and $x_k - x_j$.

The configurational energy E of $\mathcal{C} = (C_n, L)$ is defined by

$$E(\mathcal{C}) = E(C_n, L) := \frac{1}{2} \sum_{(i, j) \in \mathcal{N}} v_2(|x_i - x_j|_L) + \frac{1}{2} \sum_{(i, j, k) \in \mathcal{T}} v_3(\alpha_{ijk}), \quad (6)$$

where the factors $1/2$ are included to avoid double-counting of the interactions among same atoms. Since the energy is invariant under isometries, all statements involving E in the following are considered to hold up to isometries.

For a fixed integer $\ell > 3$, let us consider a configuration \mathcal{F} in the family \mathcal{F} . As \mathcal{F} is periodic, it can be identified with the couple (F_n, L) , where F_n is the corresponding n -cell ($n = 4m\ell$ for some $m \in \mathbb{N}$), and

$$L = L_m^\mu := m\mu \quad (7)$$

can be seen as the length of the n -sample (notice that for $m = 1$ we get the minimal period of the configuration). We note that it is natural to consider the regime $m \gg \ell$, which accounts for the fact that the nanotube is a thin and long structure. In view of (6) and (4), the energy can be written as

$$E(\mathcal{F}) = E(F_n, L_m^\mu) = \frac{n}{2} (v_2(\lambda_1) + 2v_2(\lambda_2)) + n(2v_3(\alpha) + v_3(\beta(\alpha, \gamma_\ell))). \quad (8)$$

In the particular case $\lambda_1 = \lambda_2 = 1$, we can reduce to a function \mathcal{E} of the angle α only, i.e.,

$$E(\mathcal{F}) = \mathcal{E}(\alpha) := -\frac{3}{2}n + n(2v_3(\alpha) + v_3(\beta(\alpha, \gamma_\ell))).$$

3. MAIN LOCAL MINIMALITY RESULTS

3.1. Minimization in the family \mathcal{F}_1 . Let us take the minimal period μ for a configuration in \mathcal{F} in some reference interval around the value 3, say $\mu \in (2.6, 3.1)$. We notice that 3 is the minimal period in case of unit bonds $\lambda_1 = \lambda_2 = 1$ and in case of a planar structure (which is ideally realized by $\ell = +\infty$). The minimization problem

$$\min\{E(\mathcal{F}) : \mathcal{F} = \mathcal{F}_{\lambda_1, \lambda_2, \mu}, \lambda_1 \in (0.9, 1.1), \lambda_2 \in (0.9, 1.1)\}$$

is solved by $\lambda_1 = \lambda_2 = 1$. This is clear by (8), by changing λ_1, λ_2 to 1 and by leaving α unchanged. We stress that in case $\lambda_1 = \lambda_2 = 1$, thanks to (2) and (3), we have $\mu = 2(1 - \cos \alpha)$, so that the one-parameter family \mathcal{F}_1 can be reparametrized in terms of α . Therefore, we have in principle the two equivalent minimization problems

$$\min\{E(\mathcal{F}) : \mathcal{F} \in \mathcal{F}_1, \mu \in (2.6, 3.1)\}, \quad \min\{\mathcal{E}(\alpha) : \alpha \in (\arccos(-0.3), \arccos(-0.55))\}.$$

The latter minimization problem in one variable for the map $\alpha \mapsto \mathcal{E}(\alpha)$ has been investigated in [28, Theorem 4.3]. It may require to work on a smaller interval of values of α around $2\pi/3$, depending on the specific choice of v_3 . The result in [28, Theorem 4.3] is the following:

Proposition 3.1. *There exist an open interval A and $\ell_0 \in \mathbb{N}$ only depending on v_3 such that the following holds for all $\ell \geq \ell_0$: There is a unique angle $\alpha_\ell^{\text{us}} \in A$ such that $\mathcal{E}(\alpha_\ell^{\text{us}})$ minimizes \mathcal{E} on A .*

The minimal period of the nanotube corresponding to α_ℓ^{us} is given by $\mu_\ell^{\text{us}} := 2 - 2 \cos \alpha_\ell^{\text{us}}$, so that $\mathcal{F}_{1,1,\mu_\ell^{\text{us}}}$ is the optimal configuration in \mathcal{F}_1 for μ varying in a suitable interval around 3 (depending on v_3). Nanotubes with $\mu = \mu_\ell^{\text{us}}$ will be referred to as *unstretched*, namely (*us*) *nanotubes*, as they feature unit bond lengths. In contrast, later we will consider optimal stretched nanotubes with different bond lengths.

The above result is proven easily by means of the convexity and monotonicity assumptions on v_3 around $2\pi/3$ and the properties of the function $\beta(\alpha, \gamma_\ell)$. We mention that the result in [28] further shows that neither the *polyhedral* [10, 11] nor the classical *rolled-up* [14] configuration is a local minimizer of the energy E . The polyhedral and rolled-up configurations are classical geometric definitions of carbon nanotubes, and in the zigzag case they correspond, see [28], by particular choices of α , namely

$$\alpha = 2\pi/3 \quad \text{and} \quad \alpha = \beta(\alpha, \gamma_\ell) = \arccos \left(\frac{1 - 2 \sin^2(\gamma_\ell/2)}{2 \sin^2(\gamma_\ell/2)} \right),$$

respectively.

We wish to prove that $\mathcal{F}_{1,1,\mu_\ell^{\text{us}}}$ is in fact a local minimizer with respect to any small perturbation. More precisely, if $x_1^{\text{us}}, \dots, x_n^{\text{us}}$ are the points in the n -sample of $\mathcal{F}_{1,1,\mu_\ell^{\text{us}}}$, we shall prove local minimality with respect to any configuration $\tilde{\mathcal{F}}$ that belongs to

$$\mathcal{P}_\eta = \{\tilde{\mathcal{F}} = (F_n, L) \mid F_n := \{x_1, \dots, x_n\} \text{ with } |x_i - x_i^{\text{us}}| \leq \eta, |L - m\mu_\ell^{\text{us}}| < \eta\} \quad (9)$$

for η small enough. Here, η is always assumed to be so small that the first neighboring relations of the perturbed configurations are unchanged, and no new couples of points reach a distance (modulo L) which is smaller than 1.1, that would indeed result in further contributions to the energy.

A first crucial role towards local minimality is played by adopting a energy summation strategy. We may compare two different approaches. The first one is the summation of the energy point-by-point, which leads to a very clear and simple, although incomplete proof.

3.2. Point-by-point summation of the energy. Let us denote by $\mathcal{F}^* = \mathcal{F}_{1,1,\mu_\ell^{\text{us}}}$ the unique optimal nanotube in the family \mathcal{F}_1 that is provided by Proposition 3.1, when μ varies in a suitable neighborhood of the value 3. We stress again that such neighborhood is not explicit here since it depends on the specific choice of the three-body potential v_3 which is left fairly general in our discussion. Indeed, it depends on the amplitude of the interval of strict convexity of v_3 around $2\pi/3$. We refer to [29] for a more precise quantification. When considering a perturbation $\tilde{\mathcal{F}} \in \mathcal{P}_\eta$, see (9), at each point x_i , $i = 1, \dots, n$, of the (n -sample of the) perturbed configuration we have

- three bond lengths $\bar{\lambda}_1^i, \bar{\lambda}_2^i, \bar{\lambda}_3^i$, each in a neighborhood of 1;
- two bond angles α_1^i, α_2^i : these are the perturbations of the angle α_ℓ^{us} of \mathcal{F}^* ;
- the *nonplanarity angle* γ^i , i.e., the angle between the two planes that contain respectively α_1^i and α_2^i ($\gamma^i = \pi$ in the limit planar case obtained for large ℓ , and $\gamma^i = \gamma_\ell$ if $\tilde{\mathcal{F}} \in \mathcal{F}$);
- a third bond angle β^i which can be written as a function of $\alpha_1^i, \alpha_2^i, \gamma^i$ by a simple computation, i.e., $\beta^i = \tilde{\beta}(\alpha_1^i, \alpha_2^i, \gamma^i)$, where the function $\tilde{\beta} : [\pi/2, 3\pi/4] \times [\pi/2, 3\pi/4] \times [3\pi/4, \pi] \rightarrow \mathbb{R}$ is defined by $\tilde{\beta}(\alpha_1, \alpha_2, \gamma) := 2 \arcsin \left(\sqrt{(1 - \sin \alpha_1 \sin \alpha_2 \cos \gamma - \cos \alpha_1 \cos \alpha_2)/2} \right)$.

The angle energy contribution of each point x_i of the configuration $\tilde{\mathcal{F}}$ is therefore

$$\tilde{E}(\alpha_1^i, \alpha_2^i, \gamma^i) := v_3(\alpha_1^i) + v_3(\alpha_2^i) + v_3(\tilde{\beta}(\alpha_1^i, \alpha_2^i, \gamma^i)),$$

so that the point-by-point energy summation reads

$$E(\tilde{\mathcal{F}}) = \frac{1}{2} \sum_{i=1}^n (v_2(\bar{\lambda}_1^i) + v_2(\bar{\lambda}_2^i) + v_2(\bar{\lambda}_3^i)) + \sum_{i=1}^n \tilde{E}(\alpha_1^i, \alpha_2^i, \gamma^i). \quad (10)$$

We define $\sigma_0(\gamma) := \pi - \arcsin \left(\frac{\sqrt{3}}{2 \sin(\gamma/2)} \right) < \frac{2}{3}\pi$ and collect the basic properties that arise from the study of the function \tilde{E} . For the proof we refer to [29, Section 4].

Proposition 3.2. *There exists $\gamma_0 \in \mathbb{N}$ (depending only on v_3) such that for any $\gamma \in (\gamma_0, \pi)$, the mapping $(\alpha_1, \alpha_2) \mapsto \tilde{E}(\alpha_1, \alpha_2, \gamma) = \tilde{E}(\alpha_2, \alpha_1, \gamma)$ is continuous and strictly convex on $[\sigma_0(\gamma), 2\pi/3]^2$. Denoting its unique minimizer by $(\alpha_\gamma, \alpha_\gamma)$, there holds $\alpha_\gamma \in (\sigma_0(\gamma), 2\pi/3)$. Moreover, the map $\gamma \mapsto \tilde{E}(\alpha_\gamma, \alpha_\gamma, \gamma)$ is strictly decreasing and strictly convex on (γ_0, π) .*

Now let ℓ be large enough so that $\gamma_\ell \in (\gamma_0, \pi)$. If we assume that the mean value γ_{mean} of the angles γ^i is smaller than $\gamma_\ell = \pi - \pi/\ell$, starting from (10), since $v_2 \geq -1$ and using the convexity and monotonicity properties of \tilde{E} from Proposition 3.2, letting $\alpha^i = (\alpha_1^i + \alpha_2^i)/2$ we obtain

$$\begin{aligned} E(\tilde{\mathcal{F}}) &\geq -\frac{3}{2}n + \sum_{i=1}^n \tilde{E}(\alpha_1^i, \alpha_2^i, \gamma^i) \\ &\geq -\frac{3}{2}n + \sum_{i=1}^n \tilde{E}(\alpha_{\gamma^i}, \alpha_{\gamma^i}, \gamma^i) \geq -\frac{3}{2}n + n\tilde{E}(\alpha_{\gamma_\ell}, \alpha_{\gamma_\ell}, \gamma_\ell) = E(\mathcal{F}^*). \end{aligned} \quad (11)$$

On the other hand, if $\gamma_{\text{mean}} - \gamma_\ell > 0$, there is an *angle defect* that does not allow to conclude: the last inequality fails in general. In order to get rid of the angle defect, we shall resort to a different energy summation.

3.3. Axial displacement. Let us now move forward to the case of *stretched* nanotubes, which we define, by now in the family \mathcal{F} , to be the nanotubes with $\mu \geq \mu_\ell^{\text{us}}$. For fixed $\mu \in (2.6, 3.1)$, $\mu \neq \mu_\ell^{\text{us}}$, we consider the minimization problem

$$E_{\min}(\mu) = \min \{E(\mathcal{F}_{\lambda_1, \lambda_2, \mu}) \mid \mathcal{F}_{\lambda_1, \lambda_2, \mu} \in \mathcal{F}_1, \lambda_1, \lambda_2 \in (0.9, 1.1)\}. \quad (12)$$

We obtain the following existence result which is borrowed from [18] and that generalizes Proposition 3.1.

Proposition 3.3 (Existence and uniqueness of minimizer: General case). *There exist $\ell_0 \in \mathbb{N}$ and, for each $\ell \geq \ell_0$, an open interval M^ℓ only depending on v_2, v_3 , and ℓ , with $\mu_\ell^{\text{us}} \in M^\ell$, such that for all $\mu \in M^\ell$ there is a unique pair of bondlengths $(\lambda_1^\mu, \lambda_2^\mu)$ such that $\mathcal{F}_{\lambda_1^\mu, \lambda_2^\mu, \mu}$ is a solution of the problem (12).*

In the following the minimizer is sometimes denoted for simplicity by \mathcal{F}_μ^* . Note that we have $\mathcal{F}_{\mu_\ell^{\text{us}}}^* = \mathcal{F}_{1,1,\mu_\ell^{\text{us}}}$ by Proposition 3.1. Our aim is to investigate the local minimality of \mathcal{F}_μ^* . To this end, we consider again *general* small perturbations $\tilde{\mathcal{F}}$ of \mathcal{F}_μ^* with the same bond graph, this time with prescribed stretching. Again, each atom keeps three and only three bonds, and we can identify the three neighboring atoms of the perturbed configurations with the ones for the configuration \mathcal{F}_μ^* . By $F_n^\mu = \{x_1^\mu, \dots, x_n^\mu\}$ we denote the n -cell of \mathcal{F}_μ^* so that $\mathcal{F}_\mu^* = (F_n^\mu, L_m^\mu)$ with L_m^μ as defined in (7) for $m \in \mathbb{N}$ with $n = 4m\ell$. We define *small perturbations* $\mathcal{P}_\eta(\mu)$ of \mathcal{F}_μ^* by

$$\mathcal{P}_\eta(\mu) = \{\tilde{\mathcal{F}} = (F_n, L_m^\mu) \mid F_n := \{x_1, \dots, x_n\} \text{ with } |x_i - x_i^\mu| \leq \eta\}, \quad (13)$$

where L_m^μ is defined by (7). In particular, by choosing η small enough (depending on v_2, v_3 and ℓ), the first neighboring relations among atoms do not change and still only first neighbors contribute to the energy. Moreover, we recall $E(\tilde{\mathcal{F}}) = E(F_n, L_m^\mu)$.

Starting from $\mathcal{F}_{1,1,\mu_\ell^{\text{us}}}$, we are imposing tensile stress on a nanotube by simply modifying μ . For $\mu > \mu_\ell^{\text{us}}$, we are stretching the structure with an axial traction. Note that we consider perturbations which in general preserve only the parameter $L = L_m^\mu$. This action on the structure is very general and includes for instance imposed Dirichlet boundary conditions, where only the first coordinate of the boundary atoms is prescribed. Therefore, we are in the setting of a uniaxial strain experiment where we wish to check the elastic behavior of the structure by validating the Cauchy-Born rule. Notice that prescribing a value L_m^μ (with the traction constraint $L_m^\mu > m\mu_\ell^{\text{us}}$) can be seen as prescribing the macroscopic length of the n -points sample F_n . Another example of boundary displacement that is compatible with our definition of admissible perturbations of \mathcal{F}_μ^* is the following: All atoms that lie in the leftmost section of the n -sample of \mathcal{F}_μ^* (say the ℓ atoms x such that $x \cdot \mathbf{e}_1 = 0$) keep lying on the same plane. In this case, the cell length L_m^μ is the distance between such plane and the parallel one at distance L_m^μ .

We now state the main result.

Theorem 3.4 (Local stability of minimizers). *There exist $\ell_0 \in \mathbb{N}$ and for each $\ell \geq \ell_0$ some $\mu_\ell^{\text{crit}} > \mu_\ell^{\text{us}}$ and $\eta_\ell > 0$ only depending on v_2, v_3 , and ℓ such that for all $\ell \geq \ell_0$ and for all $\mu \in [\mu_\ell^{\text{us}}, \mu_\ell^{\text{crit}}]$ we have $E(\tilde{\mathcal{F}}) > E(\mathcal{F}_\mu^*)$ for any nontrivial perturbation $\tilde{\mathcal{F}} \in \mathcal{P}_{\eta_\ell}(\mu)$ of the configuration \mathcal{F}_μ^* .*

Under prescribed and small stretchings (i.e., the value of L_m^μ is prescribed), we are proving that there exists a periodic strict-local minimizer \mathcal{F}_μ^* that belongs to the family \mathcal{F}_1 . This can be seen as a validation of the Cauchy-Born rule in this specific setting. The result applies in particular to the case $\mu = \mu_\ell^{\text{us}}$, which implies the validity of the local minimality result that we have previously discussed in Section 3.2 as a particular case. More specifically, we recall that the proof provided in Section 3.2 was incomplete, but is now completed by means of the main result of our work. We also mention that fracture has to be expected for μ above the critical value μ_ℓ^{crit} , i.e., if traction is too strong, see [18].

4. PROOF OF THE MAIN RESULT

This section provides an overview of the main lines of the proof of Theorem 3.4, following the arguments in [18]. The first point is a different energy summation with respect to the one we adopted in Section 3.2.

4.1. Cell-by-cell summation of the energy. For the configuration \mathcal{F}_μ^* from Proposition 3.3, the n -points sample F_n is made by $4m$ sections that are orthogonal to the axis of the cylinder (each with ℓ atoms). We consider a subdivision of F_n in *basic cells* (or, in the following, simply cells).

A basic cell is made of eight points which correspond to a hexagon plus its two first neighboring atoms along the parallel to the axis, see Figure 4. We denote by $\mathbf{x} = (x_1, \dots, x_8)$ the generic cell, with the ordering from Figure 4, where $x_2 - x_1$ is parallel to the axis vector \mathbf{e}_1 . Notice that the whole n -points sample contains exactly $2m\ell$ cells, that are spanned by letting the indices in the definition of $\mathcal{F}(\lambda_1, \lambda_2, \mu)$ vary as $i = 1, \dots, \ell$, $j = 1, \dots, m$, $k = 0, 1$ (while the index $l \in \{0, 1\}$ varies within the same cell).

We note that about the ends of the n -points sample, we always consider the modulo L_m^μ repetition of points in the \mathbf{e}_1 direction, i.e., we leave the interior cells and the boundary cells undistinguished. This convention is made in all the next definitions.

We define the *cell center* and the *dual center* by

$$z := \frac{x_1 + x_2}{2} \quad \text{and} \quad z^{\text{dual}} = \frac{x_2 + x_8}{2}, \quad (14)$$

respectively, see Figure 4. A small perturbation $\tilde{\mathcal{F}}$ in $\mathcal{P}_{\eta_\ell}(\mu)$ of \mathcal{F}_μ^* does not change first-neighbor relations. Therefore, we can define basic cells also in $\tilde{\mathcal{F}}$ by the identification of the points of $\tilde{\mathcal{F}}$ with the ones of \mathcal{F}_μ^* . Given the general configuration $\tilde{\mathcal{F}}$ and any of its cells \mathbf{x} , the bond lengths

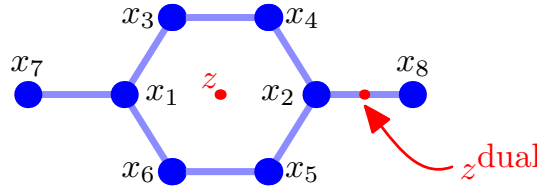


FIGURE 4. Notation for the points and the centers in the basic cell.

b_i , $i = 1, \dots, 8$, and the bond angles φ_i , $i = 1, \dots, 10$, are defined and labelled as shown in Figure 5.

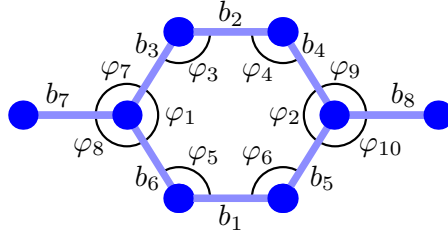


FIGURE 5. Notation for the bond lengths and angles in the basic cell.

The *cell energy* is the energy contribution of a single cell \mathbf{x} and it is defined by

$$E_{\text{cell}}(\mathbf{x}) = \frac{1}{4}(v_2(b_1) + v_2(b_2)) + \frac{1}{2} \sum_{h=3}^6 v_2(b_h) + \frac{1}{4}(v_2(b_7) + v_2(b_8)) + v_3(\varphi_1) + v_3(\varphi_2) + \frac{1}{2} \sum_{h=3}^6 v_3(\varphi_h) + \frac{1}{2} \sum_{h=7}^{10} v_3(\varphi_h). \quad (15)$$

The coefficients in the definition of E_{cell} are taken by considering that each bond that is not (approximately) parallel to \mathbf{e}_1 is contained exactly in two cells and each of the other bonds is contained in four cells, and similarly for bond angles. The computation of the energy of the cell \mathbf{x} requires the knowledge of the mapping $T: \mathbb{R}^{24} \rightarrow \mathbb{R}^{18}$ that associates to $\mathbf{x} = (x_1, \dots, x_8) \in \mathbb{R}^{24}$ the corresponding bond lengths b_i and bond angles φ_i that appear in the above right hand side.

When considering the whole n -points sample, we index its generic cells as $\mathbf{x}_{i,j,k}$, $i = 1, \dots, \ell$, $j = 1, \dots, m$, $k = 0, 1$. Therefore, the cell-by-cell summation formula for the energy reads

$$E(\tilde{\mathcal{F}}) = \sum_{i=1}^{\ell} \sum_{j=1}^m \sum_{k=0,1} E_{\text{cell}}(\mathbf{x}_{i,j,k}). \quad (16)$$

As we have seen in Section 3.2 (at least for $\mu = \mu_{\ell}^{\text{us}}$), the angle defect is the main obstacle to the conclusion of the proof of Theorem 3.4. Since the strategy is now to sum the energy cell by cell, we introduce the notion of *nonplanarity angle* of a cell, which generalizes the nonplanarity angle from Section 3.2.

For a cell $\mathbf{x} = (x_1, \dots, x_8)$ with center z and dual center z^{dual} , we denote by $\theta_l(z)$ the angle between the plane through x_1, x_3, x_4 and the one through x_1, x_5, x_6 (following the labelling of Figure 4). Similarly, we define $\theta_r(z)$ as the angle between the plane through x_2, x_3, x_4 and the one through x_2, x_5, x_6 . Moreover, $\theta_l(z^{\text{dual}})$ is the angle between the plane through x_2, x_4, x_8 and the one through x_2, x_5, x_8 . Finally, $\theta_r(z^{\text{dual}})$ is the angle between the plane through x_2, x_8, x_* and the one through x_2, x_8, x_{**} (here, x_* and x_{**} are the other two first neighboring atoms of x_8 : they belong to another cell). For the sake of definiteness, all these angles are in $[0, \pi)$.

The *nonplanarity angle* of a cell \mathbf{x} with center z and dual center z^{dual} is defined

$$\bar{\theta}(\mathbf{x}) := \frac{1}{4} (\theta_l(z) + \theta_r(z) + \theta_l(z^{\text{dual}}) + \theta_r(z^{\text{dual}})). \quad (17)$$

4.2. Symmetrization of cells. Let us now consider the basic cell of the configuration \mathcal{F}_{μ}^* that is defined by Proposition 3.3 (of course, all the basic cells of such configuration are equal). We denote it by \mathbf{x}^{kink} , where the terminology is hinting to the fact that it is kinked along the diagonal of the hexagon whose direction is \mathbf{e}_1 . Indeed, the eight points of \mathbf{x}^{kink} are contained in two planes. We can give the precise position of the eight points by fixing a reference orthogonal system $\mathbf{e}_1, \mathbf{e}_2, \mathbf{e}_3$ with the cell center coinciding with the origin. We let \mathbf{e}_1 be axis direction as usual, we let \mathbf{e}_2 be

the direction of $x_3 - x_6$, and we let $\mathbf{e}_3 = \mathbf{e}_1 \wedge \mathbf{e}_2$. The exact positions of the points in \mathbf{x}^{kink} are therefore

$$\begin{aligned} x_1^{\text{kink}} &= (-1/2 - \sigma^{\text{us}}, 0, 0), & x_2^{\text{kink}} &= (1/2 + \sigma^{\text{us}}, 0, 0), \\ x_3^{\text{kink}} &= (-1/2, \sin \alpha_\ell^{\text{us}} \sin(\gamma_\ell/2), \sin \alpha_\ell^{\text{us}} \cos(\gamma_\ell/2)), & x_4^{\text{kink}} &= x_3^{\text{kink}} + (1, 0, 0), \\ x_5^{\text{kink}} &= (1/2, -\sin \alpha_\ell^{\text{us}} \sin(\gamma_\ell/2), \sin \alpha_\ell^{\text{us}} \cos(\gamma_\ell/2)), & x_6^{\text{kink}} &= x_5^{\text{kink}} - (1, 0, 0), \\ x_7^{\text{kink}} &= (-3/2 - \sigma^{\text{us}}, 0, 0), & x_8^{\text{kink}} &= (3/2 + \sigma^{\text{us}}, 0, 0), \end{aligned}$$

where σ^{us} corresponds to the parameter in (2), γ_ℓ is defined in (5), and α_ℓ^{us} as given in Proposition 3.1. For a generic perturbation \mathbf{x} of \mathbf{x}^{kink} (resulting from a perturbation $\tilde{\mathcal{F}} \in \mathcal{P}_\eta(\mu)$), we can consider the same reference system, and by adding a rigid motion we may reduce without restriction to the following situation: the second and third components of $(x_1 + x_7)/2$, $(x_2 + x_8)/2$ (which are the dual centers of \mathbf{x} and of an adjacent cell) are equal to zero and the points x_4, x_5 lie in a plane that is parallel to the one generated by \mathbf{e}_1 and \mathbf{e}_2 .

For $y = (y^1, y^2, y^3) \in \mathbb{R}^3$ we consider $r_1(y) := (-y^1, y^2, y^3)$ and $r_2(y) := (y^1, -y^2, y^3)$. For the generic cell $\mathbf{x} = (x_1, \dots, x_8)$, we define the reflections

$$\begin{aligned} S_1(\mathbf{x}) &= (r_2(x_1) | r_2(x_2) | r_2(x_6) | r_2(x_5) | r_2(x_4) | r_2(x_3) | r_2(x_7) | r_2(x_8)), \\ S_2(\mathbf{x}) &= (r_1(x_2) | r_1(x_1) | r_1(x_4) | r_1(x_3) | r_1(x_6) | r_1(x_5) | r_1(x_8) | r_1(x_7)). \end{aligned}$$

We define the *reflected perturbations*

$$\mathbf{x}_{S_1} := \mathbf{x}_{\text{kink}}^\ell + S_1(\mathbf{x} - \mathbf{x}_{\text{kink}}^\ell), \quad \mathbf{x}_{S_2} := \mathbf{x}_{\text{kink}}^\ell + S_2(\mathbf{x} - \mathbf{x}_{\text{kink}}^\ell).$$

Indeed, since \mathbf{x} is a perturbation of \mathbf{x}^{kink} , \mathbf{x}_{S_1} (resp. \mathbf{x}_{S_2}) is the reflected perturbation with respect to the plane generated by $\mathbf{e}_1, \mathbf{e}_3$ (resp. $\mathbf{e}_2, \mathbf{e}_3$). We note that $E_{\text{cell}}(\mathbf{x}_{S_2}) = E_{\text{cell}}(\mathbf{x}_{S_1}) = E_{\text{cell}}(\mathbf{x})$ is a consequence of the symmetry of the configurations. We now define the *symmetrization of the cell* in two steps. We first perform a symmetrization with respect to the plane generated by $\mathbf{e}_1, \mathbf{e}_3$, then a symmetrization with respect to the plane generated by $\mathbf{e}_2, \mathbf{e}_3$. Of course, \mathbf{x}^{kink} is itself symmetric with respect to these two planes. We define the *symmetrized perturbations* by

$$\begin{aligned} \mathbf{x}' &:= \mathbf{x}^{\text{kink}} + \frac{1}{2} \left((\mathbf{x} - \mathbf{x}^{\text{kink}}) + S_1(\mathbf{x} - \mathbf{x}^{\text{kink}}) \right), \\ \mathcal{S}(\mathbf{x}) &:= \mathbf{x}^{\text{kink}} + \frac{1}{2} \left((\mathbf{x}' - \mathbf{x}^{\text{kink}}) + S_2(\mathbf{x}' - \mathbf{x}^{\text{kink}}) \right). \end{aligned}$$

We finally define the *symmetry defect* as the following quadratic deviation

$$\Delta(\mathbf{x}) := |\mathbf{x} - \mathbf{x}'|^2 + |\mathbf{x}' - \mathcal{S}(\mathbf{x})|^2. \quad (18)$$

We notice that the distance among the points $\frac{1}{2}(x_1 + x_7)$ and $\frac{1}{2}(x_2 + x_8)$ from the cell \mathbf{x} does not change in passing to the symmetrized configuration $\mathcal{S}(\mathbf{x})$, i.e.,

$$|(\mathcal{S}(\mathbf{x})_1 + \mathcal{S}(\mathbf{x})_7) - (\mathcal{S}(\mathbf{x})_2 + \mathcal{S}(\mathbf{x})_8)| = |(x_1 + x_7) - (x_2 + x_8)|.$$

The cell energy from (15) is expressed as a function of the 18 variables $b_1, \dots, b_8, \varphi_1, \dots, \varphi_{10}$. After taking symmetrization as above, the number of variables is reduced. In fact, let us consider those cells \mathbf{x} that are symmetrized by the above procedure. Then, possibly up to an additional rigid motion, there are lengths $\lambda, \tilde{\mu}$ and angles $\alpha_1, \alpha_2, \beta, \gamma_1, \gamma_2$ such that

$$\begin{aligned} \varphi_1 = \varphi_2 = \beta, \quad \varphi_3 = \varphi_4 = \varphi_5 = \varphi_6 = \alpha_1, \quad \varphi_7 = \varphi_8 = \varphi_9 = \varphi_{10} = \alpha_2, \\ (x_2 + x_8) - (x_1 + x_7) = 2\tilde{\mu}\mathbf{e}_1, \quad b_1 = b_2 = b_7 = b_8 = \tilde{\mu}/2 + \lambda \cos \alpha_1, \quad b_3 = b_4 = b_5 = b = 6 = \lambda \end{aligned}$$

and such that $\theta_l(z) = \theta_r(z) = \gamma_1$. Moreover, the angle between the plane through x_7, x_1, x_3 and the one through x_7, x_1, x_6 is γ_2 and the angle between the plane through x_2, x_8, x_4 and the one through x_2, x_8, x_5 is γ_2 , as well.

The notation for α_1, α_2 and β corresponds indeed to the angle notations from Section 2, and β can be expressed by the same simple trigonometric relations, namely

$$\beta = \beta(\alpha_1, \gamma_1) = 2 \arcsin \left(\sin \alpha_1 \sin \frac{\gamma_1}{2} \right) = \beta(\alpha_2, \gamma_2) = 2 \arcsin \left(\sin \alpha_2 \sin \frac{\gamma_2}{2} \right).$$

We notice that $\tilde{\mu} = \mu$ for a basic cell of a nanotube in \mathcal{F}_1 . Since we are always taking a small perturbation of an optimal configuration $\mathcal{F}_\mu^* = \mathcal{F}_{\lambda_1^\mu, \lambda_2^\mu, \mu}$, the values of all the parameters are close to the corresponding values of $\mathcal{F}_{\lambda_1^\mu, \lambda_2^\mu, \mu}$. For a highly symmetric cell as above, the cell energy (15) is equal to

$$E_{\tilde{\mu}, \gamma_1, \gamma_2}^{\text{sym}}(\lambda, \alpha_1, \alpha_2) := 2v_2(\lambda) + \frac{1}{2}v_2(\tilde{\mu}/2 + \lambda \cos \alpha_1) + \frac{1}{2}v_2(\tilde{\mu}/2 + \lambda \cos \alpha_2) \quad (19)$$

$$+ 2v_3(\alpha_1) + 2v_3(\alpha_2) + v_3(\beta(\alpha_1, \gamma_1)) + v_3(\beta(\alpha_2, \gamma_2)).$$

Therefore, the energy of highly symmetric cells as above is a function of six the variables $\alpha_1, \alpha_2, \gamma_1, \gamma_2, \lambda, \tilde{\mu}$. We further introduce the *reduced energy*, that is obtained by minimizing in the three variables $\alpha_1, \alpha_2, \lambda$, more precisely

$$E_{\text{red}}(\mu, \gamma_1, \gamma_2) := \min\{E_{\tilde{\mu}, \gamma_1, \gamma_2}^{\text{sym}}(\lambda, \alpha_1, \alpha_2) \mid \lambda \in (0.9, 1.1), \alpha_1, \alpha_2 \in (\arccos(-0.4), \arccos(-0.55))\}.$$

Here, the optimization interval are chosen for the sake of definiteness only. Since $E_{\tilde{\mu}, \gamma_1, \gamma_2}^{\text{sym}}$ is symmetric in (α_1, γ_1) and (α_2, γ_2) , then E_{red} is symmetric in γ_1 and γ_2 , i.e., $E_{\text{red}}(\mu, \gamma_1, \gamma_2) = E_{\text{red}}(\mu, \gamma_2, \gamma_1)$. We stress that the parameter μ in E_{red} plays the role of the stretching parameter, while γ_1, γ_2 are again nonplanarity measures of the cell. We borrow from [18] a general result concerning the properties of E_{red} . It can be thought as a generalization of Proposition 3.2 featuring convexity and monotonicity properties. It is proven after some lengthy explicit computations for which we refer to [18, Section 6].

Proposition 4.1. *There exists $\ell_0 \in \mathbb{N}$ and for each $\ell \geq \ell_0$ there are open intervals M^ℓ, G^ℓ only depending on v_2, v_3 and ℓ with $\mu_\ell^{\text{us}} \in M^\ell, \gamma_\ell \in G^\ell$ such that the following holds:*

1. *For each $(\mu, \gamma_1, \gamma_2) \in M^\ell \times G^\ell \times G^\ell$ there exists a unique triple $(\lambda^\mu, \alpha_1^\mu, \alpha_2^\mu)$ solving the minimization problem which defined E_{red} . Moreover, $\alpha_1^\mu = \alpha_2^\mu$ if $\gamma_1 = \gamma_2$.*
2. *E_{red} is strictly convex on $M^\ell \times G^\ell \times G^\ell$, in particular there is a constant $c'_0 > 0$ only depending on v_2 and v_3 such that $E_{\text{red}}(\mu, \gamma_1, \gamma_2) \geq E_{\text{red}}(\mu, \bar{\gamma}, \bar{\gamma}) + c'_0 \ell^{-2} (\gamma_1 - \gamma_2)^2$, with $\bar{\gamma} = (\gamma_1 + \gamma_2)/2$, for all $\mu \in M^\ell$ and $\gamma_1, \gamma_2 \in G^\ell$.*
3. *For each $\mu \in M^\ell$, the mapping $g(\gamma) := E_{\text{red}}(\mu, \gamma, \gamma)$ is decreasing on G^ℓ with $|g'(\gamma)| \leq C\ell^{-3}$ for all $\gamma \in G^\ell$ for some $C > 0$ depending only on v_3 .*
4. *The mapping $h(\mu) := E_{\text{red}}(\mu, \gamma_\ell, \gamma_\ell)$ is strictly convex on M^ℓ with $h''(\mu_\ell^{\text{us}}) > 0$ and strictly increasing on $M^\ell \cap \{\mu \geq \mu_\ell^{\text{us}}\}$.*

We note en passant that once the above properties are established, it is easy to obtain the proof of Proposition 3.3. For each $\mu \in M^\ell$ and $\gamma_1 = \gamma_2 = \gamma_\ell$, letting $\lambda_1^\mu = \mu/2 + \lambda^\mu \cos \alpha_1^\mu$ and $\lambda_2^\mu = \lambda^\mu$ with λ^μ and α_1^μ from Property 1. above, the configuration $\mathcal{F}_{\lambda_1^\mu, \lambda_2^\mu, \mu}$ is the unique minimizer of the problem (12). This can be seen by using (19) which yields along with the definition of E_{red}

$$E(\mathcal{F}_\mu^*) = E(\mathcal{F}_{\lambda_1^\mu, \lambda_2^\mu, \mu}) = 2m\ell E_{\text{red}}(\mu, \gamma_\ell, \gamma_\ell). \quad (20)$$

4.3. Estimates in terms of the symmetry defect. We denote the unique minimizer from Proposition 3.3 again by \mathcal{F}_μ^* . For a small perturbation $\tilde{\mathcal{F}} \in \mathcal{P}_\eta(\mu)$ we consider the usual identification with the n -points sample $\tilde{\mathcal{F}} = (F_n, L_m^\mu)$ and we denote the cells in F_n by the usual three index notation $\mathbf{x}_{i,j,k}$, $i = 1, \dots, \ell$, $j = 1, \dots, m$, $k = 0, 1$. Based on the properties of the reduced energy E_{red} , we are able to show that, up to a linear perturbation in terms of the symmetry defect Δ defined in (18), E_{red} bounds the cell energy E_{cell} from below.

Theorem 4.2 (Energy defect controls symmetry defect). *There exist $C > 0$ and $\ell_0 \in \mathbb{N}$ (only depending on v_2 and v_3) such that for any $\ell \geq \ell_0$ the following property holds: there exist $\eta_\ell > 0$ and an open interval M^ℓ containing μ_ℓ^{us} , such that for all $\mu \in M^\ell$ and any perturbation $\tilde{\mathcal{F}} \in \mathcal{P}_{\eta_\ell}(\mu)$, we have*

$$E_{\text{cell}}(\mathbf{x}_{i,j,k}) \geq E_{\text{red}}(|z_{i,j,k}^{\text{dual}} - z_{i,j-1,k}^{\text{dual}}|, \bar{\theta}(\mathbf{x}_{i,j,k}), \bar{\theta}(\mathbf{x}_{i,j,k})) + C\ell^{-2} \Delta(\mathbf{x}_{i,j,k}). \quad (21)$$

Here, for the definition of the dual centers we refer to (14). See (17) for the definition of $\bar{\theta}(\mathbf{x}_{i,j,k})$. The proof of the above theorem requires some hard computations and it represents a

key step towards the proof of the main result. Indeed, thanks to Theorem 4.2, we are able to quantify the energy gain in passing from a highly non-symmetric configuration to a symmetrized one, in terms of the symmetry defect Δ . Thanks to this gain, it will be possible to get rid of the angle defect that arises when taking the average nonplanarity angle of the rolled-up structure, as seen in Section 3.2. The proof of Theorem 4.2 is based on a detailed study of the convexity properties of the mapping $T : \mathbb{R}^{24} \rightarrow \mathbb{R}^{18}$ which associates the position (x_1, \dots, x_8) of the points of a cell to the associated bond lengths b_1, \dots, b_8 and bond angles $\varphi_1, \dots, \varphi_{10}$. For the proof we refer to [18, Section 7].

When resorting to a cell-by-cell energy summation, the nonplanarity angles are defined by (17). It is also possible to prove the following estimate in terms of Δ . For the proof, we refer to [18, Section 5].

Theorem 4.3 (Symmetry defect controls angle defect). *There is a universal constant $c > 0$ such that for $\eta > 0$ small enough and for all $\tilde{\mathcal{F}} \in \mathcal{P}_\eta(\mu)$ with cells $\mathbf{x}_{i,j,k}$ and $\Delta(\mathbf{x}_{i,j,k}) \leq \eta$ we have*

$$4 \sum_{j=1}^m \sum_{i=1}^{\ell} \sum_{k=0,1} \bar{\theta}(\mathbf{x}_{i,j,k}) \leq 4m(2\ell - 2)\pi + c \sum_{j=1}^m \sum_{i=1}^{\ell} \sum_{k=0,1} \Delta(\mathbf{x}_{i,j,k}).$$

The left hand side above is equal to $4m(2\ell - 2)\pi$ if $\tilde{\mathcal{F}} \in \mathcal{F}_1$.

4.4. Proof of the main theorem. After having collected the main technical auxiliary results in the previous subsections, we conclude by giving the main line of the proof of Theorem 3.4.

Let ℓ_0 be large enough and let M^ℓ be an open interval containing μ_ℓ^{us} such that Proposition 4.1 and Theorem 4.2 hold for all $\ell \geq \ell_0$ and $\mu \in M^\ell$. Also let G^ℓ be the interval from Proposition 4.1 and let $\mu_\ell^{\text{crit}} > \mu_\ell^{\text{us}}$ be such that $[\mu_\ell^{\text{us}}, \mu_\ell^{\text{crit}}] \subset M^\ell$. Given $\ell \geq \ell_0$ and $\mu \in [\mu_\ell^{\text{us}}, \mu_\ell^{\text{crit}}]$, we consider a nontrivial perturbation $\tilde{\mathcal{F}} \in \mathcal{P}_{\eta_\ell}(\mu)$, see (13), with η_ℓ as in Theorem 4.2. We denote again the generic cells of the n -points sample by $\mathbf{x}_{i,j,k}$, its center by $z_{i,j,k}$ and its dual center by $z_{i,j,k}^{\text{dual}}$. The nonplanarity angle $\bar{\theta}(\mathbf{x}_{i,j,k})$ is defined in (17).

Furthermore, we introduce the *average cell length* and the *average non-planarity angle*, namely

$$\bar{\mu} = \frac{1}{2m\ell} \sum_{j=1}^m \sum_{i=1}^{\ell} \sum_{k=0,1} |z_{i,j,k}^{\text{dual}} - z_{i,j-1,k}^{\text{dual}}|, \quad \bar{\theta} = \frac{1}{2m\ell} \sum_{j=1}^m \sum_{i=1}^{\ell} \sum_{k=0,1} \bar{\theta}(\mathbf{x}_{i,j,k})$$

respectively. By taking the perturbation parameter η_ℓ small enough, we can assume that $\Delta(\mathbf{x}_{i,j,k})$ satisfies the assumptions of Theorem 4.3 for all i, j, k . We deduce that

$$\bar{\theta} \leq \frac{1}{8m\ell} \left(4m(2\ell - 2)\pi + c \sum_{j=1}^m \sum_{i=1}^{\ell} \sum_{k=0,1} \Delta(\mathbf{x}_{i,j,k}) \right) \leq \gamma_\ell + \frac{c}{8m\ell} \sum_{j=1}^m \sum_{i=1}^{\ell} \sum_{k=0,1} \Delta(\mathbf{x}_{i,j,k}). \quad (22)$$

We note that we can not exclude that $\bar{\theta} > \gamma_\ell$, so that an angle defect appears as seen in (11). However, we have obtained a bound in terms of the symmetry defect.

If η_ℓ is small, $|z_{i,j,k}^{\text{dual}} - z_{i,j-1,k}^{\text{dual}}| \in M^\ell$ and $\bar{\theta}(\mathbf{x}_{i,j,k}) \in G^\ell$ for all i, j, k . By Theorem 4.2 there is $C > 0$ (depending only on v_2, v_3) such that for each cell (21) holds. We now take advantage of the cell-by-cell energy summation (16): By (21), by (16), and by using Property 2. of Proposition 4.1, we find

$$E(\tilde{\mathcal{F}}) = \sum_{i=1}^{\ell} \sum_{j=1}^m \sum_{k=0,1} E_{\text{cell}}(\mathbf{x}_{i,j,k}) \geq 2m\ell E_{\text{red}}(\bar{\mu}, \bar{\theta}, \bar{\theta}) + C\ell^{-2} \sum_{i=1}^{\ell} \sum_{j=1}^m \sum_{k=0,1} \Delta(\mathbf{x}_{i,j,k}). \quad (23)$$

On the other hand, by (22), (23), and by Property 3. of Proposition 4.1 we deduce that for some $C' > 0$ only depending on v_3 there holds

$$E(\tilde{\mathcal{F}}) \geq 2m\ell E_{\text{red}}(\bar{\mu}, \gamma_\ell, \gamma_\ell) + (C\ell^{-2} - C'\ell^{-3}) \sum_{j=1}^m \sum_{i=1}^{\ell} \sum_{k=0,1} \Delta(\mathbf{x}_{i,j,k}). \quad (24)$$

Notice that the estimates in the last two lines are analogous to the ones in (11) as they make use of minimality, convexity, and monotonicity. We stress that, in contrast to (11), after passing to the energy of a symmetrized configuration (which is measured by E_{red}) we have a gain in terms of the symmetry defect. On the other hand, the angle defect is also estimated in terms of the symmetry defect, and from (24) we see that the latter can be overcome if ℓ is large enough.

In order to conclude, we need to pass from $\bar{\mu}$ to μ with a monotonicity argument. Notice that only small perturbations with prescribed value of $L_m^\mu = m\mu$ are allowed, see (13). Therefore, for fixed i and k we have

$$m\mu = L_m^\mu = \left| \sum_{j=1}^m z_{i,j,k}^{\text{dual}} - z_{i,j-1,k}^{\text{dual}} \right| \leq \sum_{j=1}^m |z_{i,j,k}^{\text{dual}} - z_{i,j-1,k}^{\text{dual}}|.$$

As a consequence, by taking the sum over all i and k , we get $\bar{\mu} \geq \mu \geq \mu_\ell^{\text{us}}$. Then, from (24) and by Property 4. of Proposition 4.1, we find

$$E(\tilde{\mathcal{F}}) \geq 2m\ell E_{\text{red}}(\mu, \gamma_\ell, \gamma_\ell) + C''\ell^{-2} \sum_{i=1}^{\ell} \sum_{j=1}^m \sum_{k=0,1} \Delta(\mathbf{x}_{i,j,k}) \quad (25)$$

for ℓ_0 sufficiently large and a constant $C'' > 0$ depending on v_2, v_3 . We stress that the assumption $\mu \geq \mu_\ell^{\text{us}}$, i.e., the nanotube is unstretched or under traction but not under compression, is crucial for the application of the monotonicity property from Property 4. of Proposition 4.1.

By (20) and (25) we get $E(\tilde{\mathcal{F}}) \geq E(\mathcal{F}_\mu^*)$. Eventually, it is not difficult to revisit the above estimates and to get the strict inequality $E(\tilde{\mathcal{F}}) > E(\mathcal{F}_\mu^*)$ since the perturbation is nontrivial.

ACKNOWLEDGEMENTS

This work was supported by the Deutsche Forschungsgemeinschaft (DFG, German Research Foundation) under Germany's Excellence Strategy EXC 2044 -390685587, Mathematics Münster: Dynamics–Geometry–Structure. E.M. acknowledges support from the MIUR-PRIN project No 2017TEXA3H and from the INDAM-GNAMPA 2019 project “*Trasporto ottimo per dinamiche con interazione*”. P.P. is partially supported by the Austrian Science Fund (FWF) project P 29681 and by the Vienna Science and Technology Fund (WWTF), the city of Vienna, and Berndorf Privatstiftung through Project MA16-005.

The authors would like to thank Marco Morandotti and Davide Zucco, organizers of the conference *Analysis and applications: contribution from young researchers*, held at the Politecnico di Torino on 8-9 April 2019, where the content of this paper was presented.

REFERENCES

- [1] P. M. Agrawal, B. S. Sudalayandi, L. M. Raff, R. Komandur. Molecular dynamics (MD) simulations of the dependence of C-C bond lengths and bond angles on the tensile strain in single-wall carbon nanotubes (SWCNT), *Comp. Mat. Sci.* 41 (2008), 450–456.
- [2] N. L. Allinger. *Molecular structure: understanding steric and electronic effects from molecular mechanics*, Wiley, 2010.
- [3] M. Arroyo, T. Belytschko. Continuum mechanics modeling and simulation of carbon nanotubes, *Meccanica*, 40 (2005), 455–469.
- [4] C. Bajaj, A. Favata, P. Podio-Guidugli. On a nanoscopically-informed shell theory of single-wall carbon nanotubes, *Eur. J. Mech. A Solids*, 42 (2013), 137–157.
- [5] D. W. Brenner. Empirical potential for hydrocarbons for use in stimulating the chemical vapor deposition of diamond films, *Phys. Rev. B*, 42 (1990), 9458–9471.
- [6] B. R. Brook, R. E. Brucoleri, B. D. Olafson, D. J. States, S. Swaminathan, M. Karplus. CHARMM: A program for macromolecular energy, minimization, and dynamics calculations, *J. Comp. Chem.* 4 (1983), 187–217
- [7] G. X. Cao, X. Chen. The effects of chirality and boundary conditions on the mechanical properties of single-wall carbon nanotubes, *Int. J. Solid. Struct.* 44 (2007), 5447–5465.
- [8] M. Clark, R. D. Cramer III, N. Van Opdenbosch. Validation of the general purpose tripos 5.2 force field, *J. Comp. Chem.* 10 (1989) 982–1012.
- [9] J. Clayden, N. Greeves, S. G. Warren. *Organic chemistry*, Oxford University Press, 2012.

- [10] B. J. Cox, J. M. Hill. Exact and approximate geometric parameters for carbon nanotubes incorporating curvature, *Carbon*, 45 (2007), 1453–1462.
- [11] B. J. Cox, J. M. Hill. Geometric structure of ultra-small carbon nanotubes, *Carbon*, 46 (2008), 711–713.
- [12] E. Davoli, P. Piovano, U. Stefanelli. Wulff shape emergence in graphene. *Math. Models Methods Appl. Sci.* 26 (2016), 12:2277–2310.
- [13] B. G. Demczyk et al. Direct mechanical measurement of the tensile strength and elastic modulus of multiwalled carbon nanotubes, *Mat. Sci. Engrg.* A334 (2002), 173–178.
- [14] M. S. Dresselhaus, G. Dresselhaus, R. Saito. Physics of carbon nanotubes, *Carbon*, 33 (1995), 883–891.
- [15] A. Favata, P. Podio-Guidugli. A new CNT-oriented shell theory, *Eur. J. Mech. A/Solids*, 35 (2012), 75–96.
- [16] A. Favata, A. Micheletti, P. Podio-Guidugli. A nonlinear theory of prestressed elastic stick-and-spring structures, *J. Engrg. Sci.* 80 (2014), 4–20.
- [17] A. Favata, P. Podio-Guidugli. A shell theory for carbon nanotube of arbitrary chirality. *Shell and membrane theories in mechanics and biology*, 155–167, Adv. Struct. Mater., 45, Springer, Cham, 2015.
- [18] M. Friedrich, E. Mainini, P. Piovano, U. Stefanelli. Characterization of Optimal Carbon Nanotubes Under Stretching and Validation of the Cauchy-Born Rule, *Arch. Rational Mech. Anal.* 231 (2019) 465–517.
- [19] M. Friedrich, P. Piovano, U. Stefanelli. The geometry of C_{60} : a rigorous approach via Molecular Mechanics, *SIAM J. Appl. Math.* 76 (2016), 2009–2029.
- [20] M. Friedrich, U. Stefanelli. Graphene ground states, *Z. Angew. Math. Phys.* 69:70 (2018).
- [21] W. F. van Gunsteren, H. J. C. Berendsen. *Groningen Molecular Simulation (GROMOS) Library Manual*, BIOMOS b.v., Groningen, 1987.
- [22] F. Han, Y. Azdoud, G. Lubineau. Computational modeling of elastic properties of carbon nanotube/polymer composites with interphase regions. Part I: Micro-structural characterization and geometric modeling, *Comp. Mat. Sci.* 81 (2014), 641–651.
- [23] V. K. Jindal, A. N. Imtani. Bond lengths of armchair single-walled carbon nanotubes and their pressure dependence, *Comp. Mat. Sci.* 44 (2008), 156–162.
- [24] A. Krishnan, E. Dujardin, T. W. Ebbesen, P. N. Yianilos, M. M. J. Treacy. Young’s modulus of single-walled nanotubes, *Phys. Rev. B*, 58 (1998), 14013–14019
- [25] E. G. Lewars. *Computational Chemistry*, 2nd edition, Springer, 2011.
- [26] F. Li, H. M. Cheng, S. Bai, G. Su, M. S. Dresselhaus. Tensile strength of single-walled carbon nanotubes directly measured from their macroscopic ropes. *Appl. Phys. Lett.* 77, 3161 (2000)
- [27] X. Li, W. Yang, B. Liu. Bending induced rippling and twisting of multiwalled carbon nanotubes, *Phys. Rev. Lett.* 98 (2007), 205502–205505.
- [28] E. Mainini, H. Murakawa, P. Piovano, U. Stefanelli. Carbon-nanotube geometries: analytical and numerical results, *Discrete Contin. Dyn. Syst. Ser. S*, 10 (2017), 141–160.
- [29] E. Mainini, H. Murakawa, P. Piovano, U. Stefanelli. Carbon-nanotube geometries as optimal configurations, *Multiscale Model. Simul.*, 15 (2017), 4:1448–1471.
- [30] E. Mainini, U. Stefanelli. Crystallization in carbon nanostructures, *Comm. Math. Phys.* 328 (2014), 2:545–571.
- [31] S. L. Mayo, B. D. Olafson, W. A. Goddard. DREIDING: a generic force field for molecular simulations, *J. Phys. Chem.* 94 (1990), 8897–8909.
- [32] P. Poncharal, Z. L. Wang, D. Ugarte, W. A. de Heer. Electrostatic deflections and electro-mechanical resonances of carbon nanotubes, *Science*, 283 (1999), 1513–1516.
- [33] A. K. Rappé, C. L. Casewit. *Molecular mechanics across chemistry*, University Science Books, Sausalito, CA, 1997.
- [34] A. Rochefort et al. Electrical and mechanical properties of distorted carbon nanotubes, *Phys. Rev. B*, (1999) 60:13824–13830.
- [35] C. Q. Ru. Axially compressed buckling of a doublewalled carbon nanotube embedded in an elastic medium, *J. Mech. Phys. Solids*, 49 (2001), 1265–1279.
- [36] R. S. Ruoff, D. Qian, W. K. Liu. Mechanical properties of carbon nanotubes: theoretical predictions and experimental measurements, *C. R. Physique*, 4 (2003), 993–1008.
- [37] F. H. Stillinger, T. A. Weber. Computer simulation of local order in condensed phases of silicon, *Phys. Rev. B*, 8 (1985), 5262–5271.
- [38] J. Tersoff. New empirical approach for the structure and energy of covalent systems. *Phys. Rev. B*, 37 (1988), 6991–7000.
- [39] J. Tersoff. Empirical interatomic potential for carbon, with applications to amorphous-carbon. *Phys. Rev. Lett.*, 61 (1988), 2879–2882.
- [40] J. Tersoff. Modeling solid-state chemistry - interatomic potentials for multicomponent systems. *Phys. Rev. B*, 39 (1989) 5566–5568.
- [41] M. M. J. Treacy, T. W. Ebbesen, J. M. Gibson. Exceptionally high Young’s modulus observed for individual carbon nanotubes, *Nature*, 381 (1996), 678–680.
- [42] X. Wang, X. Wang, J. Xiao. A non-linear analysis of the bending modulus of carbon nanotubes with rippling deformations, *Compos. Struct.* 69 (2005), 315–321.
- [43] J. H. Warner, N. P. Young, A. I. Kirkland, G. A. D. Briggs. Resolving strain in carbon nanotubes at the atomic level, *Nature Materials*, 10 (2011), 958–962.

- [44] P. K. Weiner, P. A. Kollman. AMBER: Assisted model building with energy refinement. A general program for modeling molecules and their interactions, *J. Comput. Chem.* 2 (1981), 287–303.
- [45] X. Wang, Q. Li, J. Xie, Z. Jin, J. Wang, Y. Li, K. Jiang, S. Fan. Fabrication of Ultralong and Electrically Uniform Single-Walled Carbon Nanotubes on Clean Substrates, *Nano Lett.* 9 (2009), 9: 3137–3141.
- [46] B. I. Yakobson, P. Avouris. Mechanical Properties of Carbon Nanotubes. In: Dresselhaus M.S., Dresselhaus G., Avouris P. (eds) Carbon Nanotubes. Topics in Applied Physics, vol 80. Springer, Berlin, Heidelberg (2001).
- [47] B. I. Yakobson, C. J. Brabec, J. Bernholc. Nanomechanics of carbon tubes: instabilities beyond linear response, *Phys. Rev. Lett.* 76 (1996), 2511–2514.
- [48] M.-F. Yu, B.S. Files, S. Arepalli, R.S. Ruoff. Tensile loading of ropes of single wall carbon nanotubes and their mechanical properties, *Phys. Rev. Lett.* 84 (2000), 5552–5555.
- [49] M.-F. Yu, O. Lourie, M. J. Dyer, K. Moloni, T. F. Kelly, R. S. Ruoff. Strength and Breaking Mechanism of Multiwalled Carbon Nanotubes Under Tensile Load. *Science* 287 (2000), 637–640.
- [50] D.-B. Zhang, T. Dumitriča. Elasticity of ideal single-walled carbon nanotubes via symmetry-adapted tight-binding objective modeling, *Appl. Phys. Lett.* 93 (2008) 031919.
- [51] R. Zhang, Y. Zhang, F. Wei. Controlled Synthesis of Ultralong Carbon Nanotubes with Perfect Structures and Extraordinary Properties, *Acc. Chem. Res.* 50 (2017), 2:179–189.

(Manuel Friedrich) APPLIED MATHEMATICS MÜNSTER, UNIVERSITY OF MÜNSTER, EINSTEINSTRASSE 62, 48149 MÜNSTER, GERMANY

E-mail address: manuel.friedrich@uni-muenster.de

URL: <https://www.uni-muenster.de/AMM/Friedrich/index.shtml>

(Edoardo Mainini) DIPARTIMENTO DI INGEGNERIA MECCANICA, ENERGETICA, GESTIONALE E DEI TRASPORTI (DIME), UNIVERSITÀ DEGLI STUDI DI GENOVA, VIA ALL'OPERA PIA 15, I-16145 GENOVA, ITALY

E-mail address: mainini@dime.unige.it

URL: <http://www.dime.unige.it/it/users/edoardo-mainini>

(Paolo Piovano) FACULTY OF MATHEMATICS, UNIVERSITY OF VIENNA, OSKAR-MORGENSTERN-PLATZ 1, A-1090 VIENNA, AUSTRIA

E-mail address: paolo.piovano@univie.ac.at

URL: http://www.mat.univie.ac.at/~piovano/PaoloSamp_Dist_CorrPiovano.html